Field Survey and Preliminary Modeling of the Wewak, Papua New Guinea Earthquake and Tsunami of 9 September 2002

Jose C. Borrero[1], James Bu[2], Christine Saiang[2], Burak Uslu[1], John Freckman[3], Brandon Gomer[4], Emile A. Okal[4], and Costas E. Synolakis[1]

INTRODUCTION

At 18:44 UTC on 8 September 2002 (04:44 on 9 September, local time), a strong earthquake (m_b 6.5, M_S 7.8; hereafter "PNG02") occurred off the northern coast of the East Sepik Province of Papua New Guinea ("PNG"; see Figure 1) and triggered a moderate tsunami that was observed along 300 km of the northern PNG coast. This event is of particular interest since it occurred only 120 km east-southeast of the earthquake of 17 July 1998 (m_b 5.9, M_S 7.0; hereafter "PNG98"), which triggered a devastating tsunami with a death toll exceeding 2,100 (Kawata *et al.*, 1999).

The two earthquakes generated very different patterns of damage and destruction. PNG02 was strongly felt from Sissano Lagoon in the west to Murik Lakes in the east, a distance of 250 km (Figure 2); five people were killed, and several more injured, by the collapse of structures. On the other hand, its tsunami inundated several coastal villages but caused only a small amount of damage to beachfront structures. No one was killed by the tsunami, although four people nearly drowned. By contrast, PNG98 caused very little earthquake damage, mostly concentrated in the epicentral area near the Serai sawmill, where a few log stacks collapsed and rockslides were observed along strongly weathered cliffs. No one was killed by the earthquake. However, the tsunami triggered by PNG98 was exceptionally devastating, with waves reaching heights of 15 m, destroying three villages and severely damaging many others along a 40-km stretch of coast. Over the past 100 years, only the 1933 Sanriku, Japan tsunami had a higher death toll (estimated at 3,000).

Successful modeling of the 1998 tsunami could be achieved only by hypothesizing that the earthquake triggered a 4 km^3 landslide, an assumption corroborated by a number of subsequent geological and geophysical observations (Tappin *et al.*, 1999; Heinrich *et al.*, 2000; Synolakis *et al.*, 2002; Sweet and Silver, 2003; Okal, 2003). The purpose of the present paper is to report the preliminary findings of seismological studies of PNG02 and the results of field work in the aftermath of the event by the University of PNG and by the International Tsunami Survey Team. We also present preliminary numerical simulations of the tsunami. We conclude that its characteristics can be modeled without invoking any large-scale underwater landslide.

From the standpoint of tsunami awareness and mitigation, we note that since the PNG98 disaster, the local population has been sensitized to tsunami hazard, and, as a result, evacuation was the rule rather than the exception in 2002. This probably contributed to the lack of tsunami casualties. As PNG02 was widely felt and did produce a noticeable and relatively damaging tsunami, it may have had a positive effect, namely that of reminding the local population that tsunamis are always likely to occur after a strong earthquake.

TECTONIC FRAMEWORK

The tectonic framework of the northern PNG coast is relatively complex, as most recently summarized by Tregoning (2002). On a very coarse scale, the island of New Guinea sits at the boundary between the large Pacific and Australian Plates, which are involved in an oblique collision, the convergence vector striking S70°W at a rate of 11.1 cm/yr (DeMets *et al.*, 1990). On a finer scale, the identification of spreading centers and transform fault segments along the Bismarck Sea Seismic Lineation (BSSL) led to the early recognition of a South Bismarck Plate (Johnson and Molnar, 1972). More recently, GPS data have suggested the existence of an independent North Bismarck Plate, rotating at a slow but detectable rate (0.3°/Myr) with respect to the Pacific Plate, but whose rigidity remains debatable (Tregoning, 2002). While the BSSL is well defined, intersecting the PNG coastline in the immediate vicinity of Wewak, the northern boundary of the North Bismarck Plate, the Manus Trench, must be extrapolated to the coast, in the vicinity of the Indonesia-PNG border at 141°E. Under this interpretation, both PNG98 and PNG02 occurred along the boundary between the Australian Plate and the North Bismarck Plate, where

1. Department of Civil Engineering, University of Southern California
2. Department of Geology, University of Papua New Guinea
3. Marine Facilities Division, California State Lands Commission
4. Department of Geological Sciences, Northwestern University

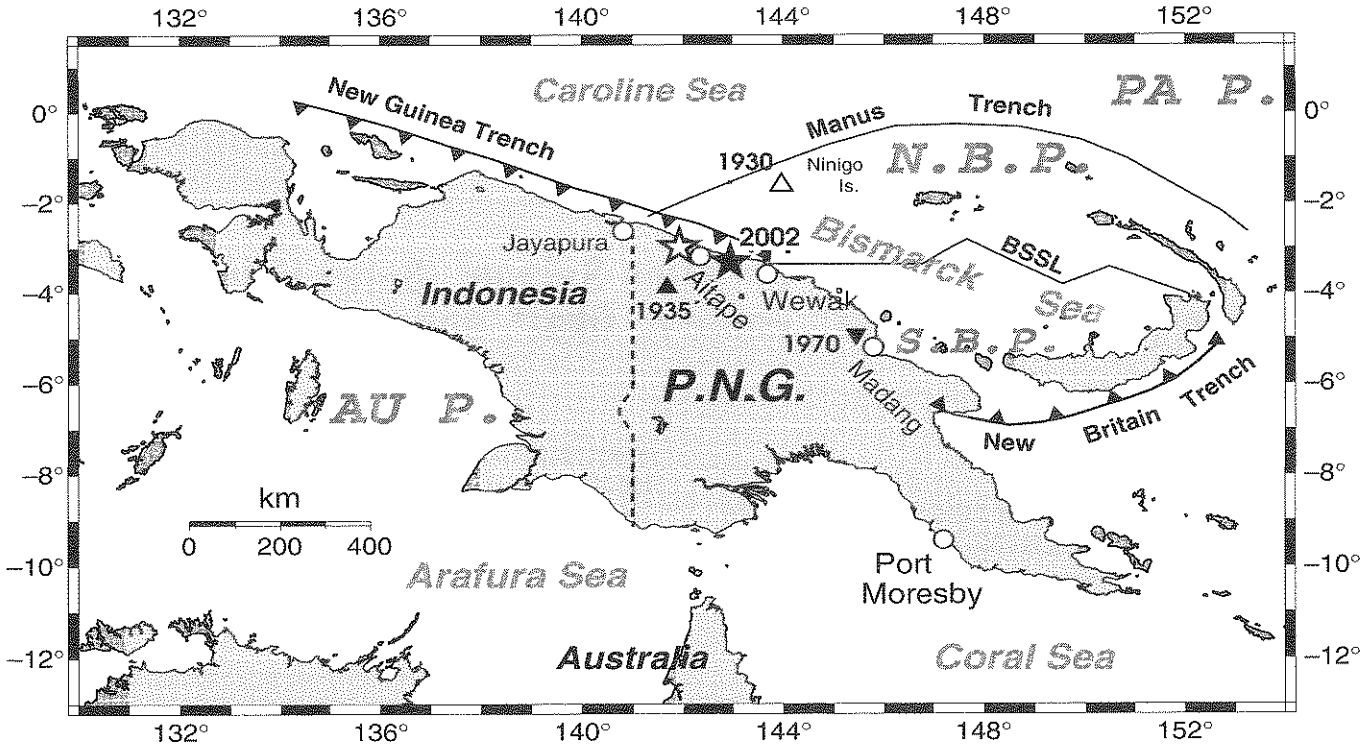

▲ **Figure 1.** Map of New Guinea showing the principal tectonic features in the area, after Tregoning (2002). The North Bismarck (N.B.P.) and South Bismarck (S.B.P.) platelets are separated by the Bismarck Sea Seismic Lineation (BSSL). The large stars identify the epicenters of PNG98 (open) and PNG02 (solid). Triangles show the relocated epicenters of the earthquakes of 1930 (Ninigo Islands, open), 1935 (Toricelli Range, solid), and 1970 (Madang, inverted).

oblique convergence takes place at a rate of 10.8 cm/yr and an azimuth of S71°W.

Large earthquakes occur regularly along the Sandaun coast of PNG, many of which have triggered substantial tsunamis (Everingham, 1977). Of particular interest to us in the Aitape-Wewak region are the following historical events:

- 15 December 1907, which was followed by very slow subsidence, doubling the size of Sissano Lagoon (Neuhauss, 1911). Solov'ev *et al.* (1986) list the epicenter as 3.1°S, 142.5°E (shown as an open triangle on Figure 2), but the origin of this estimate is unclear.
- 23 December 1930, whose tsunami inflicted significant damage in the Ninigo Islands along the Manus Trench and on the Sandaun coast of mainland New Guinea. Using the technique of Wysession *et al.* (1991), we have relocated the event at 1.60°S, 143.98°E, as shown by the open triangle in Figure 1.
- 20 September 1935, which triggered only a minor wave at Aitape. This earthquake was assigned a large magnitude (M 7.9) by Gutenberg and Richter (1954), which we have confirmed through a mantle magnitude measurement (M_m 8.06 or $M_0 = 1.1 \times 10^{28}$ dyn-cm) using a Love wave record at De Bilt (Okal and Talandier, 1990). This event relocates about 110 km inland at 3.88°S, 141.69°E (solid triangle in Figure 1). Its focal depth converges to 57 km if left floating; however, it is poorly constrained with inverted depths ranging from 0 to 182 km under Wysession *et al.*'s (1991) Monte Carlo algorithm. It is probable that the earthquake is deeper than normal, and the weak tsunami almost certainly reflects its inland location within the Toricelli range.
- 22 February 1951, which triggered a lone wave in Aitape. We have relocated the earthquake at 3.30°S, 142.17°E, 25 km southwest of Aitape (solid triangle in Figure 2).
- 31 October 1970, further east in the vicinity of Madang (inverted triangle in Figure 1). This was a strike-slip event described in detail by Everingham (1975), for which we estimate a moment of slightly less than 10^{27} dyn-cm, based on mantle magnitudes at Pasadena. A local tsunami reaching 4 m was reported, probably generated by underwater slumping as suggested by its short period of only a few minutes, and by the failure of two communication cables under turbidity currents, 15 to 40 km offshore.

The catastrophic PNG98 tsunami was described in detail by Kawata *et al.* (1999) and Synolakis *et al.* (2002); details of the field surveys are given in Borrero (2002) and Davies *et al.* (2003). This event constituted a landmark in modern tsunami research in that the effects of the waves as measured in the field (amplitude and distribution of wave heights, damage assessment) could not be explained by the seismic source using accepted models of earthquake-generated tsunamis. For that reason, the original 1998 surveyors hypothesized that an

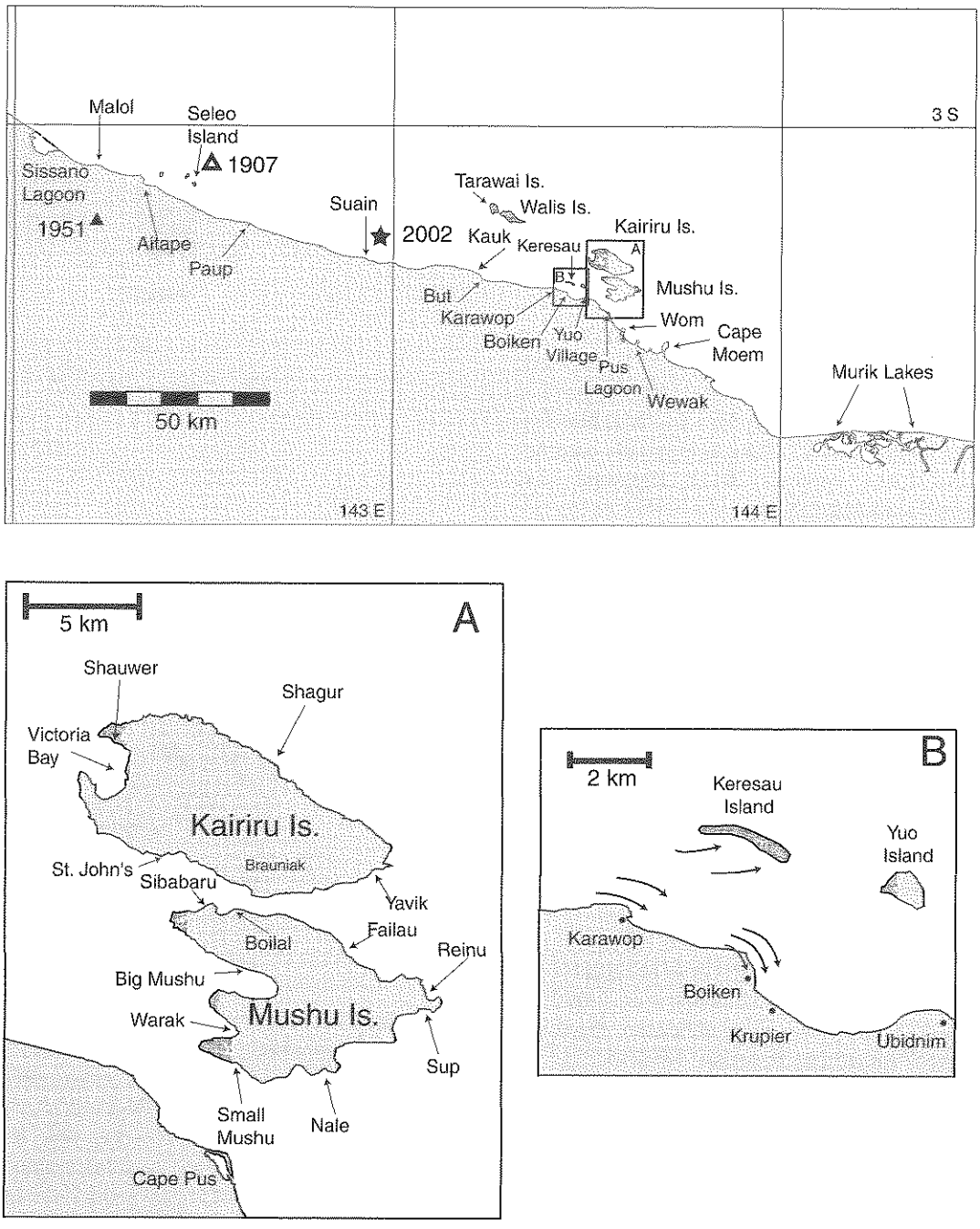

▲ **Figure 2.** Location map for the post-tsunami survey along the Sandaun coast of PNG. Also shown are the 2002 epicenter (star), the relocated epicenter of the 1951 event (solid triangle), and the unrelocated epicenter quoted by Solov'ev *et al.* (1986) for the 1907 event (open triangle). Panel A shows a close-up of the islands of Kairiru and Mushu and panel B the region around Boiken. Ubidnim Village and the Hawain River are undiscernable from Yuo on the scale of the map.

underwater landslide or slump triggered by the earthquake was responsible for generating the locally destructive waves (Synolakis *et al.*, 1998). Subsequent offshore surveys (Tappin *et al.*, 1999; Sweet and Silver, 2003) confirmed the presence of a "fresh" underwater slump, a likely candidate for the tsunami source. Hydroacoustic investigations of *T* phases generated during the 1998 event (Okal, 2003) and hydrodynamic simulation (Synolakis *et al.*, 2002) further support the model of a slump-generated tsunami.

In this general framework, since PNG02 occurred only 120 km from the site of PNG98, and because a tsunami was reported, we felt it important to conduct a detailed survey of the effects of the 2002 event in an attempt to understand better the difference in generation mechanisms between the two events. The results are presented below.

SEISMOLOGICAL ASPECTS

The PDE hypocentral location for PNG02 is 3.30°S, 142.95°E, with a depth of 13 km, a location approximately halfway between Aitape and Wewak, and within a few kilometers of the shoreline (Figure 2). Focal mechanisms available in the immediate aftermath of the earthquake included Harvard's QUICK CMT solution (strike $\phi = 110°$, dip $\delta = 25°$, slip $\lambda = 52°$) and the "Fast Moment" from NEIC ($\phi = 80°$, $\delta = 78°$, $\lambda = 6°$, a pure strike-slip geometry). We retain the final Harvard solution ($\phi = 106°$, $\delta = 34°$, $\lambda = 43°$), whose angular distance from the QUICK CMT is only 11° in the formalism of Kagan (1991). The CMT moment (2.97×10^{27} dyn-cm) is consistent with a fault length L = 72 km, a width W = 36 km, and a slip Δu = 2.1 m under classical scaling laws (Geller, 1976). Using comparable parameters, Matsuyama (pers. comm., 2002) suggested that observed crustal deformations (in particular, uplift on the offshore islands of Walis, Tarawai, Kairiru, and Mushu) show better agreement with the shallow-dipping fault plane mechanism than with its steeply dipping conjugate. The former mechanism is readily interpreted as expressing the convergence of the Australian and North Bismarck Plates at an azimuth of S68°W. The shallow-dipping solution also agrees well with the distribution of aftershock locations available from the PDE bulletin.

The source slowness of PNG02 was investigated using the formalism of Newman and Okal (1998), applied to 20 digital stations well distributed in azimuth. As shown in Figure 3, the resulting parameter $\Theta = \log_{10}(E^E/M_0)$, where E^E is the estimated radiated seismic energy, is robust and its average value (–4.82) is essentially that predicted by scaling laws (–4.90). We conclude that PNG02 features an essentially normal source behavior and in particular does not exhibit the trend toward slowness detected by Synolakis *et al.* (2002) in the case of PNG98, let alone the energy deficiency characteristic of the so-called "tsunami earthquakes" ($\Theta \leq -5.75$).

POSTEARTHQUAKE FIELD SURVEYS

Immediately after the event, a team from the University of Papua New Guinea conducted a series of surveys in the epicentral area. Their purpose was to assess earthquake damage for the governmental relief efforts as well as to collect preliminary data on the earthquake and tsunami (Davies, 2002; Davies *et al.*, 2002). These early surveys were instrumental in focusing and guiding the tsunami survey team which arrived two weeks later.

The preliminary surveys showed that it was the earthquake, rather than the tsunami, that caused most of the damage and all the fatalities (five killed, several more injured). Shaking was responsible for the collapse of buildings and, most critically for the local population, for toppling many water tanks and severing a water main in Wewak.

Earthquake damage was more severe in areas underlain by unconsolidated sediment, where extensional faults developed, notably at Kauk and Ubidnim, near the mouth of the Hawain River. On the east and north coasts of Kairiru Island many landslides were triggered, and fissures with displacements of 10–30 cm opened as a result of incipient failure on steep slopes. Liquefaction of unconsolidated subsurface sediments was common from Kauk eastward and was most pronounced at Ubidnim, where large blowout holes developed and water and sand spouted 3–5 m into the air. At Ubidnim

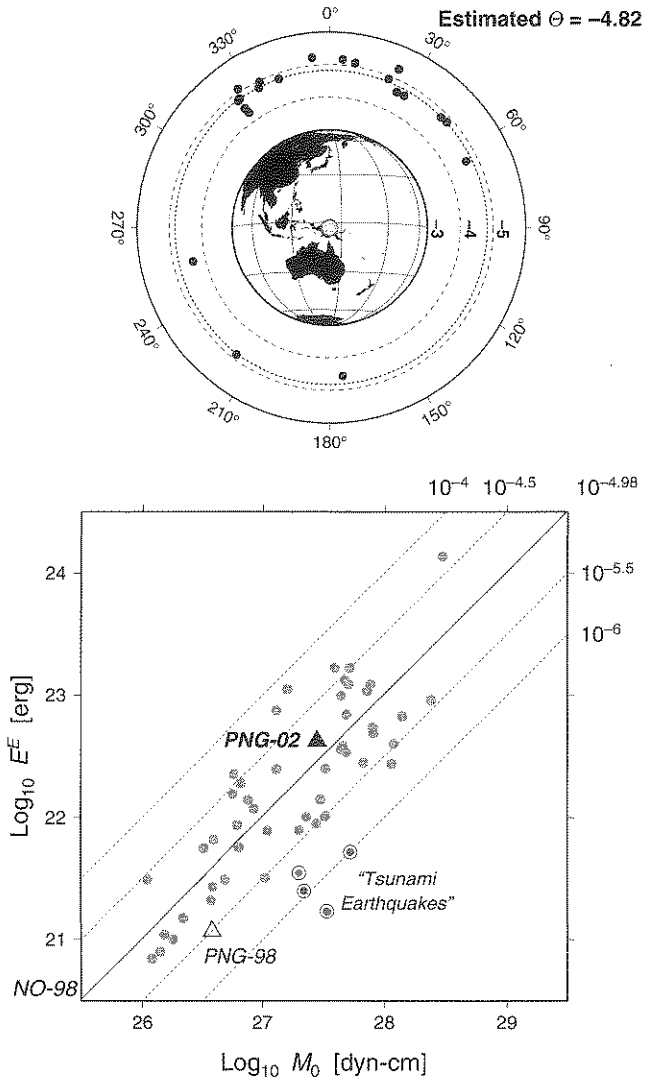

▲ **Figure 3.** *Top:* Azimuthal distribution of the slowness parameter $\Theta = \log_{10}(E^E/M_0)$ for the PNG02 earthquake, as computed for twenty teleseismic stations. The individual values are plotted radially with concentric dashed lines ranging from $\Theta = -3$ (at the boundary of the map) to $\Theta = -6$ (at the outside circle). The average value of Θ, –4.82, is shown as the dotted line. *Bottom:* Estimated energy E^E plotted vs. moment M_0 (after Newman and Okal [1998]). The faint dotted lines correspond to constant values of Θ, the solid line to its average value (–4.98) for Newman and Okal's data set. The large triangles refer to the two recent PNG events. Note that PNG02 falls within the mainstream population. By contrast, the bull's eye symbols characterize the energy deficiency found in the source of the recent "tsunami earthquakes."

and other villages, liquefied sediment moved laterally and upward to fill open water wells completely.

Brick school buildings collapsed at Hawain but little other damage was observed to Western-style buildings. About 10% of village dwellings, built of bush materials, collapsed completely and another 20% were damaged to some degree. A roaring noise approaching Wewak from the west-northwest was reported before and during the earthquake. Night fishermen also reported a bright blue-green glow in the sky above Kreer, immediately south of Wewak.

Road approaches at several bridges subsided by 10–20 cm, and a landslide blocked the coast highway at Hawain. In Wewak, the water main was severed in two places, one where a lightweight frame carrying the pipe across a river collapsed, the second where a buried section of concrete pipe broke following motion of unconsolidated material around it.

The outer islands—Tarawai, Walis, Kairiru, and Mushu—were elevated by 30–40 cm. Eyewitnesses on Tarawai reported that the uplift happened some time after the earthquake, in two stages an hour apart. It caused the emergence, at midtide, of reefs and wave-cut platforms and the setting of new strand lines on beaches. Swamp lands on Tarawai, Walis, and Mushu partly drained and the water level in wells dropped. This may become a severe problem, as the swamp lands are important as a source of sago, a staple food.

In summary, the level of damage, such as the collapse of brick buildings, the toppling of water tanks, and the occurrence of sand and mud spouts, generally corresponds to Modified Mercalli Intensity VIII, perhaps locally reaching IX in Wewak with the rupture of an underground water main.

POST-TSUNAMI FIELD SURVEYS

The International Tsunami Survey Team (ITST), comprising researchers from the United States and UPNG, visited the area from 26 to 30 September and focused solely on tsunami effects.

Field Methods

The goals of the ITST were to document *inundation*, the horizontal extent of water penetration, and *runup*, the maximum vertical elevation of the land flooded; and to collect information on the human impact of the tsunami, especially in comparison with the 1998 event. A variety of standard tsunami field survey techniques (*e.g.*, Tsuji *et al.*, 1995; Okal *et al.*, 2002) were used, including:

1. Observing and recording water height and inundation indicators such as debris, water marks on soil and buildings, elevation of damage such as broken windows and stripped roofs, and debris and sand deposited on stairs, upper floors, and roofs. Care was taken in interpreting watermarks as they relate to episodes when the water was still enough to leave a mark, almost always at levels less than peak water height.
2. Interviewing eyewitnesses. It is easy to misinterpret debris and strand lines that may be caused by high tides and storm waves unless corroborated as a tsunami deposit by eyewitnesses. Human perception during catastrophic events can be skewed, however. Whenever possible, team members spoke with several groups of people to ensure a consistent story, with most interviews recorded on video tape for permanent archiving.
3. Surveying profiles, using optical equipment, across beaches from the water line to the maximum inland extent of inundation.
4. Interviewing government officials and aid workers and collecting reports, maps, photographs, and other materials pertinent to the tsunami.

Field Observations

The field data collected by the ITST are listed in Table 1 and plotted in Figure 4, with locations detailed in Figure 2. All runup data are given relative to the tide level at the time of the earthquake, but coseismic uplift is not taken into account.

The highest runup (~5 m) was measured on the south side of Victoria Bay on Kairiru Island. High runup values were concentrated on the west-facing bays of Kairiru and Mushu and on the mainland to the south and west. Runup and inundation tapered off gradually to the east and west of these maxima. Due to the possible amplification of runup heights by the offshore island bays, the field data in Figure 4 have been divided into mainland and island subsets.

Western Region

West of Aitape, tsunami activity was minimal; residents felt the earthquake very strongly but did not report extreme water motions. At Sissano Lagoon, a site devastated in 1998, one fisherman reported strong surges flowing through the mouth of the lagoon, persisting for a few hours after the earthquake.

At Aitape, the tsunami was noticed as a series of surges that flowed up the Aitape River and spilled over the banks. They advanced as a bore up the river, raising the level 60 to 90 cm, and reached the bottom of the road bridge 300 m inland at a height of ~1 m. Up to twelve distinct surges were reported, the first and largest coming 30 minutes after the earthquake, then continuing for up to 2 hours. Further east on the mainland, witnesses at Paup reported two surges reaching over 2 m above sea level. In contrast, at the next site eastward, Suain, residents reported no positive surge, but they did note that the ambient tide level seemed "lower than normal" for several days after the earthquake.

Central Mainland Region

The area most affected by the tsunami extended from Kauk to Cape Moem and included the offshore islands. The mainland village of Kauk experienced a positive surge of nearly 1.8 m, while 15 km to the east at But no wave activity was reported. The data at both locations are robust, as verified at Kauk through a clear inundation line and an eyewitness, while at But, the entire population, awake at the time of the

TABLE 1

Location	Latitude (S)	Longitude (E)	Positive Wave?	Runup (cm)	Inundation Distance (m)
Small Mushu	3.439°	143.555°	Y	80.0	15.0
Warak	3.427°	143.559°	Y	150.0	90.0
Big Mushu 1	3.404°	143.561°	Y	146.0	52.5
Big Mushu 2	3.404°	143.561°	Y	178.0	37.0
Big Mushu 3	3.404°	143.562°	Y	115.0	20.0
Big Mushu Bay	3.099°	143.574°	Y	196.5	63.5
St. John's	3.363°	143.537°	Y	135.5	10.0
Victoria Bay, south	3.340°	143.509°	Y	500.8	28.0
Victoria Bay, back	3.342°	143.513°	Y	230.0	58.0
Burwan	3.333°	143.521°	Y	230.0	78.5
Brauniak	3.378°	143.575°	Y	273.5	46.0
Sissano, east spit	3.033°	142.092°	N	—	n/a
Malol	3.100°	142.233°	??	20.0	10.0
Aitape 1 (w. of river)	3.142°	142.350°	Y	157.2	51.5
Aitape 2 (w. of river)	3.142°	142.351°	Y	119.2	16.7
Aitape (bridge)	3.142°	142.346°	Y	103.5	n/a
Aitape 3 (e. of river)	3.142°	142.350°	Y	109.0	71.0
Seleo Island	3.151°	142.489°	Y	122.0	10.0
Paup	3.242°	142.593°	Y	228.9	30.0
Suain	3.343°	142.941°	Y	20.0	5.0
Walis Island 1	3.239°	143.296°	N	—	n/a
Walis Island 2	3.239°	143.296°	N	—	n/a
Yuo Village 1	3.437°	143.504°	Y	54.0	58.5
Yuo Village 2	3.438°	143.505°	Y	108.7	82.3
Yuo Village 3	3.437°	143.503°	Y	94.7	27.3
Yuo Village 4	3.437°	143.502°	Y	59.5	34.4
Tarawai	3.217°	143.268°	Y	—	n/a
Keresau 1	3.393°	143.443°	Y	107.5	13.2
Keresau 2	3.393°	143.444°	Y	92.3	24.5
Keresau 3	3.393°	143.445°	Y	117.9	41.0
Keresau 4	3.390°	143.440°	Y	107.5	10.0
Shauer	3.325°	143.521°	Y	216.8	81.2
Murik Lakes	3.786°	144.141°	Y	83.5	46.1[1]
Boiken 1	3.426°	143.451°	Y	226.3	93.5
Boiken 2	3.429°	143.451°	Y	255.5	80.9
Boiken 3	3.431°	143.452°	Y	183.5	72.1
Krupier	3.435°	143.456°	Y	179.5	85.0
Karawop	3.415°	143.421°	Y	255.5	13.3
Karawop Plantation	3.413°	143.419°	Y	183.5	77.5
But	3.387°	143.230°	N	0.0	0.0
Kauk	3.360°	143.161°	Y	179.5	51.1

TABLE 1 (Continued)

Location	Latitude (S)	Longitude (E)	Positive Wave?	Runup (cm)	Inundation Distance (m)
Wom Peninsula	3.518°	143.596°	Y	66.7	39.6
Wom Beach	3.519°	143.588°	Y	205.4	59.7
Pus Lagoon	3.485°	143.559°	?	—	n/a
Karau Village, Murik	3.783°	144.467°	Y	100.5	33.0[1]
Kaup, Murik	3.800°	144.000°	Y	128.0	18.3[2]
Moem, Wewak 1	3.555°	143.705°	Y	123.0	25.0
Moem, Wewak 2	3.558°	143.703°	Y	119.0	6.0
Wewak Beach	3.578°	143.625°	Y	92.0	21.0
Boram Hospital 1	3.558°	143.632°	Y	119.3	11.0
Boram Hospital 2	3.558°	143.632°	Y	134.0	10.0
Boram Beach	3.571°	143.629°	Y	64.0	10.0
Nale 1	3.441°	143.583°	Y	27.9	31.0
Nale 2	3.441°	143.584°	Y	105.6	31.1
Sup	3.421°	143.630°	N	—	n/a
Shagur 1	3.318°	143.553°	Y	236.7	9.0
Shagur 2	3.318°	143.553°	Y	313.6	20.1
Yavik	3.667°	143.592°	Y	140.0	13.6
Chokoilal	3.385°	143.543°	Y	189.0	35.3
Boilal Beach	3.384°	143.558°	Y	124.7	47.0
Bagatai	3.386°	143.570°	Y	263.3	36.4
Failau 1	3.390°	143.587°	Y	144.0	37.5
Failau 2	3.390°	143.587°	Y	111.0	71.3

1. At Murik and Karau, the inundation distance is the total distance across the sand bar from the sea to the lagoon. The villages were flooded due to a simultaneous rise of water level in both the lagoon and the sea.
2. At Kaup, the inundation distance is from the sea to the highest point of the berm. The village was flooded from the lagoon side for 100+ m behind the berm, however.

earthquake for a religious ceremony, reported neither a positive wave nor any kind of flooding.

The situation changes considerably at the next sites to the east. At Boiken, on the eastern side of a small headland (Figure 2B), the tsunami was very strong: The residents felt the earthquake, then observed the withdrawal of the sea with the seafloor exposed as if "looking down a hill." Three distinct surges were reported, the first one coming in from the sea while the second one came from the west, sweeping across the headland and along the shoreline through the village (Figures 2B and 5). Two individuals were entrained by the flow and nearly drowned. Maximum runup was measured at 1.8 to 2.5 m and inundation distances at 75 to 190 m.

At Krupier (Figure 5), the surge came in directly from the north, overtopped the 1.8-m berm, and flowed through the village and into the swamp behind it. Flow depths in the village were 40 to 60 cm, *i.e.*, lower than the floors of the stilted huts, whose interiors were not wetted. Inundation of 80 m was measured to the edge of the swamp, but this is a minimum value since the surge continued inland through the swamp.

Slightly smaller runup was measured to the west at Karawop (1.8 m) and to the east at Yuo Village (0.5 to 1.0 m), at the mouth of the Hawain River (Figure 2). Even though Yuo Village is on a headland very similar in size and shape to the one at Boiken only 10 km to the west, the tsunami was much smaller and less energetic than at Boiken.

Keresau, Walis, and Tarawai Islands

Keresau, directly offshore of the Boiken headland and closest to the mainland, experienced some flooding and positive runup (0.9 to 1.1 m), with inundation from 10 to 30 m. Along the north shore of Keresau, there were no eyewitnesses and there was no reliable indication of a positive wave.

Further offshore on Walis and Tarawai, residents reported only a withdrawal of the sea, which stayed out for many hours, but no positive wave. The reefs were exposed some 500 m offshore. Both islands were clearly uplifted, an estimated 50 cm at the eastern end of Tarawai and between 30 and 50 cm on Walis, based on a comparison of current and previous high-tide levels.

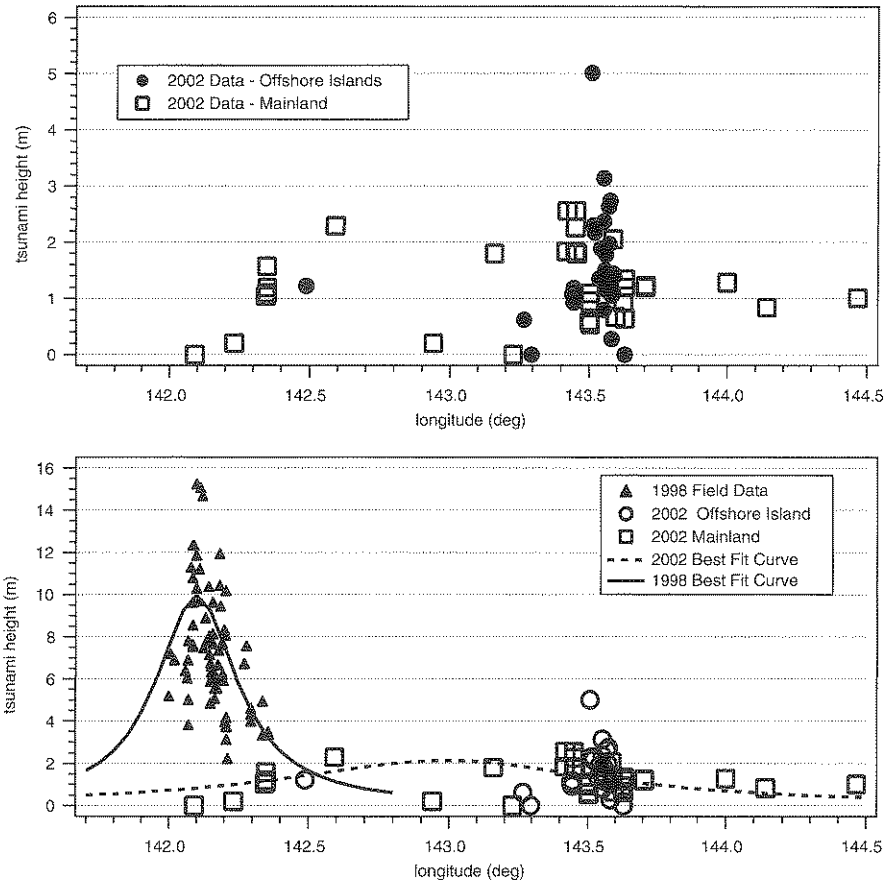

▲ **Figure 4.** *Top*: Tsunami runup plotted as a function of longitude along the coastline. Because of the larger bays affecting runup on the offshore islands, data from the latter are given different symbols. *Bottom:* Comparison with runup data from PNG98, plotted on the same scale. Also shown are curves of type (1), best fit to both data sets (excluding island points). Note the strong difference in the aspect ratios of the two distributions, arguing for a different tsunami-generation mechanism.

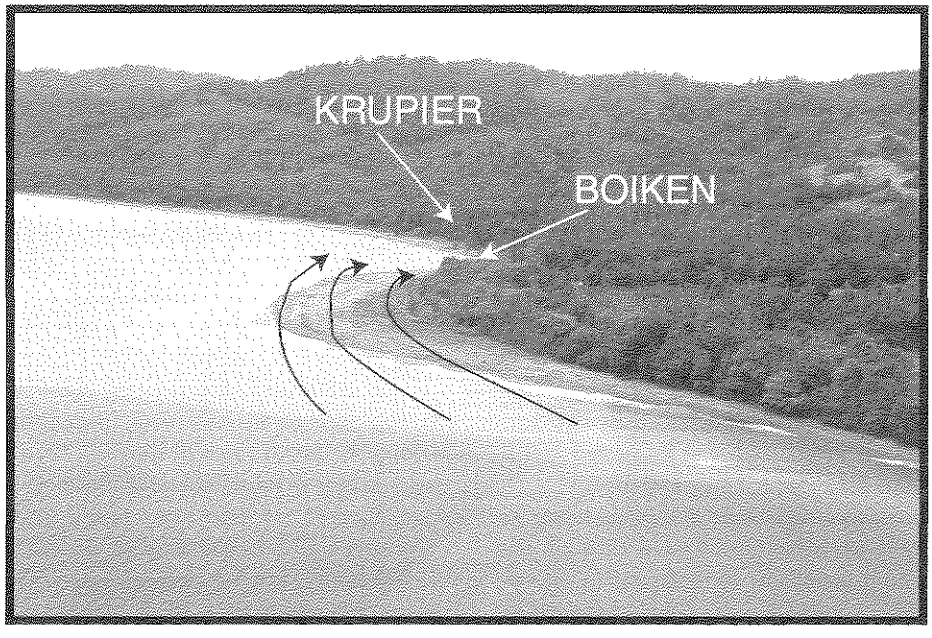

▲ **Figure 5.** Photograph of the headland at Boiken. The arrows show the direction of approach of the second and most destructive wave, as reported by local residents. Locations of Boiken and Krupier villages are also shown; the distance from the headland to Krupier is about 1 km.

Mushu and Kairiru Islands

To the northwest of Wewak, these two large islands (Figure 2A) were greatly affected by the earthquake and tsunami. Kairiru is rugged and steep, with a maximum elevation of 760 m, while Mushu is much flatter, reaching only 120 m. Both have west-facing bays that trapped the tsunami and amplified the runup, up to 5.5 m on the south side of Victoria Bay on Kairiru. The village of Shauer on the north side of the bay was flooded by the wave, which penetrated more than 100 m and reached a height of 2.1 m. On Mushu, the village of Warak was inundated to a distance of 100 m and a runup of 1.5 m, with two structures damaged. Sand deposition was extensive, with a uniform layer of white beach sand 1 to 2 cm thick overlain atop a layer of thick black mud.

East to Wewak

On the Wom Peninsula, a village was inundated; to the west, at Cape Pus, one resident reported surges flowing in and out of the lagoon and noted water flowing out of cracks in the ground near the shore. In Wewak, surges flowed over the seawall, onto the coastal road along the main beach and up a drainage canal, for up to a few hours after the earthquake, as also observed at Aitape and Cape Pus. East of Wewak at Moem, several locations were surveyed with a runup of ~1.2 m. There was evidence of sand deposition from the tsunami overtopping a sea wall and flooding across a coastal road. No data were taken between Moem and the Murik Lakes area due to accessibility and time constraints.

Murik Lakes

In the far eastern region of the survey area, the Murik Lakes are a series of lagoons with barrier islands and very low topographic relief; the region is regularly flooded by strong ocean swells. Three locations were surveyed, with similar accounts of the sea rising above the berm (~1 m) while the lagoon level also rose, flooding the villages from inland, to a depth of 30 cm to 1 m.

DISCUSSION

Overall the tsunami effects were moderate. There were no deaths or serious injuries caused by the waves, but there was some minor damage to structures already weakened or partially collapsed after the strong earthquake. Figure 4 shows a long, low distribution of runup values along the coast. Following Okal *et al.* (2002) and Hoffmann *et al.* (2002), we fit a bell curve of the type

$$h = \frac{b}{\left(\frac{(x-c)}{a}\right)^2 + 1}$$

to the runup heights h as a function of distance along the coast, x, excluding data points on the islands; a, b, and c are empirically determined constants. The aspect ratio (b/a) of the curve is 2.6×10^{-5}, which compares favorably with other tsunamis interpreted as generated by pure dislocation sources, *e.g.*, Camana, Perú (2001), 4×10^{-5}; and Nicaragua (1992), 3.3×10^{-5} (Okal *et al.*, 2002).

In contrast, similar calculations performed on the field data collected after PNG98 yielded an aspect ratio of 4.8×10^{-4}, 18 times greater than for PNG02 and implying a much steeper and narrower distribution. This suggests that the two events had distinctly different generation mechanisms and further supports the interpretation of the 1998 tsunami as caused by an underwater slump (Kawata *et al.*, 1999; Tappin *et al.*, 1999; Synolakis *et al.*, 2002). A comparison between the two data sets is also shown in Figure 4.

Tsunami Modeling

As was done for PNG98, our preliminary modeling efforts used available fault-plane solutions to compute a field of seafloor deformations, which were then input as initial conditions for the tsunami simulations. Based on focal parameters derived from the Harvard CMT solution in the geometry of the shallow-dipping source (see above), we used Okada's (1985) algorithm to compute the static displacement of the ocean floor, as shown in Figure 6. Over Kairiru and Mushu Islands, the deformation contours predict an uplift of up to 65 cm, consistent with local observations. They also correctly predict substantial uplift (40 to 50 cm) in the area of Walis and Tarawai Islands.

To perform the simulations, a 300-m (approx. 10-arcsec) grid was developed based on publicly available 2-minute bathymetry, topography, and coastline data. The raw data were smoothed using an 8-point moving average filter to minimize steep topographic gradients which can lead to numerical instabilities. Even in the absence of bathymetric data on a finer scale, some information can be gleaned from such coarse grid simulations.

The tsunami simulation was performed using the MOST (Method of Splitting Tsunami) code (Titov and Gonzalez, 1997; Titov and Synolakis, 1998; Borrero *et al.*, 2002). This is a fully nonlinear shallow-water simulation with a moving shoreline algorithm to predict water motions and overland flow at the land-sea boundary. The seismic deformations are assumed to be instantaneous, since they occur much more rapidly than the water waves would propagate out of the deformed area.

We present both the runup along the shoreline (Figure 6) and time histories of water surface fluctuations at selected points in the flow field (Figure 7). The computed runup values from the preliminary seismic dislocation model underpredict the relevant field data (points recorded on the mainland). This result is not surprising since preliminary, simple fault solutions with uniform slip over the entire fault plane can locally underpredict individual values of tsunami runup in the near field (Geist, 2002). The distribution of the runup matches the observed data quite well, however. Furthermore, the arrival times predicted by the simulations agree with the

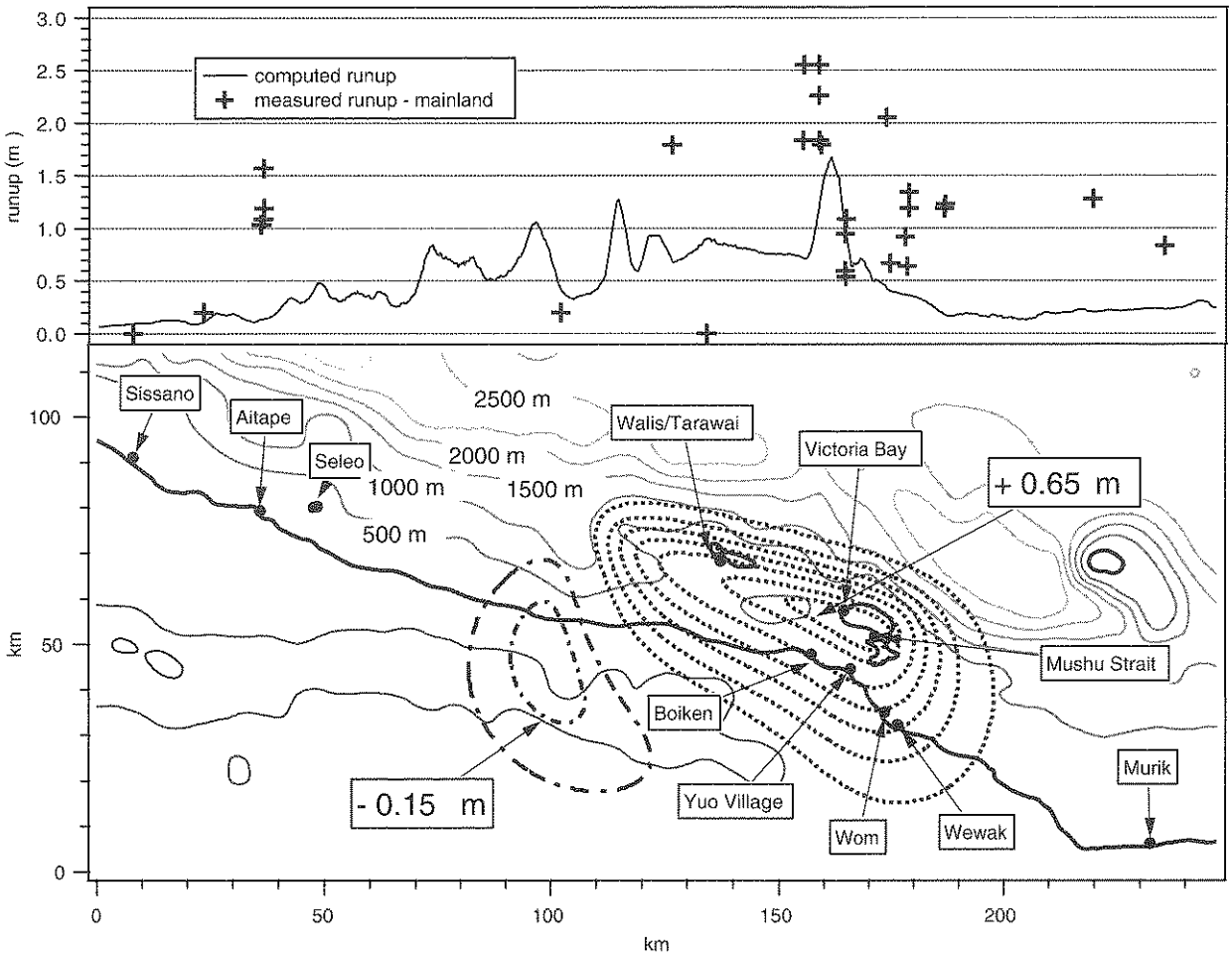

▲ **Figure 6.** *Top:* Amplitude of simulated runup along the mainland coast, plotted as a function of longitude. Crosses identify individual data from Table 1. *Bottom:* Seismic deformation computed using Okada's (1985) algorithm. Bathymetric contour intervals are noted on the figure. Equal-uplift contours are drawn (dotted lines) at intervals of 0.1 m (with an additional contour at 0.65 m); equal-subsidence contours are shown as dash-dot lines at –0.10 m and –0.15 m. Note maximum uplift on land reaching 65 cm at Kairiru Island.

limited timing information obtained in the field. Residents in Aitape reported surges in the river "a half hour" after the quake, while residents on the offshore islands gave shorter times, from zero to 15 minutes. This is reflected in the gauge records in Figure 7, panels A and B.

The simulation appears to capture the higher runup values observed on the mainland coast near Boiken (Figure 6, upper panel), indicating probable bathymetric focusing. Figure 7C, for a wave gauge located offshore Boiken, shows a large withdrawal occurring between 15 and 25 minutes after the earthquake, in general agreement with reports from local residents, who had walked from the village to the headland, a distance of 500 m, shortly after the earthquake and then witnessed the withdrawal of the sea. One could reasonably assume that 15 minutes had passed between the time of the earthquake and the time that they observed the withdrawal at the headland. Regardless, extreme caution should be employed when assessing the simulation results due to the cumulative uncertainties present in the dislocation source and the model bathymetry.

CONCLUSION

The level of earthquake damage from PNG02 identified by the field surveys generally corresponds to MM Intensities VIII and perhaps locally IX, approximately two units above that from PNG98. In very general terms, this would be consistent with the difference of 0.9 unit observed in body-wave magnitudes (6.8 as opposed to 5.9), under the assumption of seismic source scaling (Toppozada, 1975). This suggests that the source of PNG02 was a classic, "textbook", seismic dislocation, a conclusion supported by the regular value of its slowness parameter Θ and the adequate predictions of uplift along the coast and the neighboring islands.

The ITST field survey confirms that the effects of the 2002 tsunami were moderate, especially relative to the devastation wrought by the 1998 event. Our data set of runup heights surveyed along the mainland coast features an aspect ratio characteristic of tsunamis generated by seismic dislocations, and as much as 18 times less than for PNG98. Based on seismological models of the earthquake source, our pre-

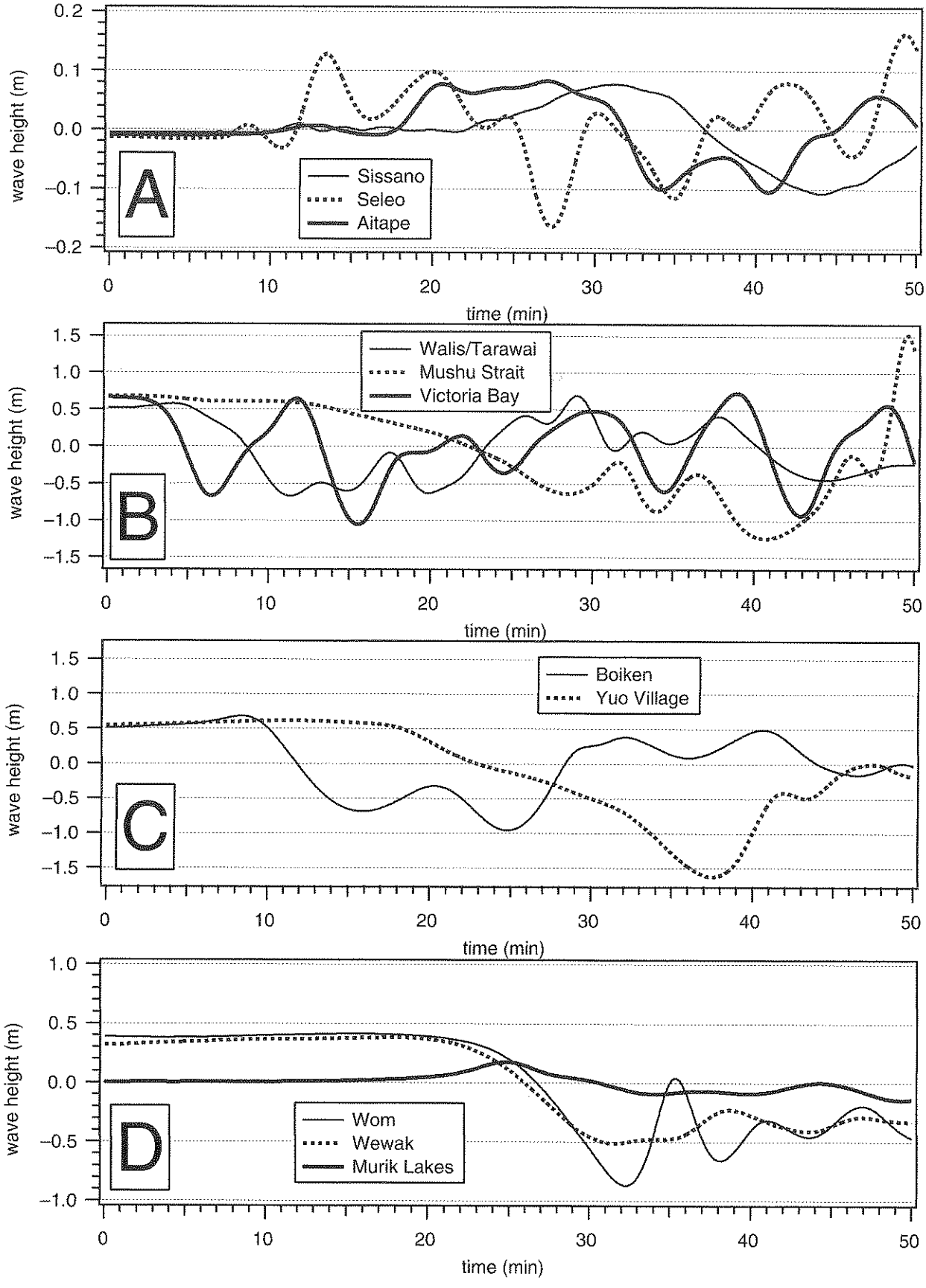

▲ **Figure 7.** Simulated water surface time series at locations indicated in Figure 6.

liminary simulation efforts underestimate the amplitude of runup but correctly predict its observed lateral distribution; such a fit had been impossible to achieve in the case of PNG98 using any dislocation source compatible with seismological observations. This combination of results reinforces the interpretation of the 1998 tsunami as having been generated by an underwater landslide, itself triggered by the earthquake.

It is particularly remarkable that, despite runup heights locally reaching 5 m, the tsunami claimed no victims. This is certainly due in large part to a responsible reaction on the part of the coastal population, namely fleeing inland or to higher ground upon feeling the shaking or noticing early water motions. It is gratifying to conclude that education or simple awareness can effectively mitigate tsunami hazard in the wake of significant earthquakes. Indeed, local residents almost unanimously referred to memories of the 1998 disaster as motivating and guiding their responses. The people of PNG should be commended for this behavior; we hope the 2002 event will serve as an additional reminder to the coastal residents of the omnipresent tsunami danger upon occurrence of an earthquake.

ACKNOWLEDGMENTS

We are deeply grateful for the openness and hospitality of the local residents who aided us despite the recent disaster. We thank Prime Minister Michael Somare for taking the time to meet with the survey team during his visit to Wewak. Professor Hugh Davies of UPNG assisted with logistics, and his first reconnaissance surveys were instrumental to the success of our mission. Special thanks are reserved for Mr. Francis Saunat, who worked tirelessly in the field over the course of several days. We were also greatly aided by Mr. Pius Munkaje and Mr. Ray Seeto of the Wewak Provincial Disaster Committee, who assisted with logistics and boat transportation to the offshore islands. Mr. David Inau was a superb helicopter pilot and a great source of information. EAO thanks Ralph Archuleta for a discussion of seismic intensities during a transatlantic flight. The support of the National Science Foundation under Grant Number CMS-0244537 is gratefully acknowledged. Seismological data were obtained from the IRIS, ISC, and NEIC Web databases. Bathymetric data were provided by Masafumi Matsuyama of Central Research Institute of Electric Power Industry, Japan. An earlier version of this paper benefited from a thoughtful review. Figures 1 and 3 were drafted using the *GMT* software (Wessel and Smith, 1991).

REFERENCES

Borrero, J. C. (2002). *Analysis of the Tsunami Hazard in Southern California*, Ph.D. dissertation, University of Southern California, Los Angeles.

Borrero, J. C., H. L. Davies, B. Uslu, E. A. Okal, and C. E. Synolakis (2002). Preliminary modeling of tsunami waves generated by the earthquake of 9 September 2002 offshore of northern Papua New Guinea, *Eos, Transactions of the American Geophysical Union* **83**, F1005 (abstract).

Davies, H. L. (2002). Field survey report of the September 9, 2002 Wewak earthquake, *International Tsunami Information Center Newsletter.*

Davies, H. L., J. M. Davies, R. C. B. Perembo, and W. Y. Lus (2003). The Aitape 1998 tsunami: Reconstructing the event from interviews and field mapping, *Pure and Applied Geophysics* **160** (in press).

Davies, H. L. and the Wewak Survey Team (2002). Preliminary results of the field survey, 2002 PNG earthquake at Wewak, *Eos, Transactions of the American Geophysical Union* **83**, F1005 (abstract).

DeMets, D. C., R. G. Gordon, D. F. Argus, and S. Stein (1990). Current plate motions, *Geophysical Journal International* **101**, 425–478.

Everingham, I. B. (1975). Seismological report on the Madang earthquake of 31 October 1970 and aftershocks, *Bureau of Mineral Resources, Geology, and Geophysics Report* 176, Canberra, 45 pp.

Everingham, I. B. (1977). *Preliminary Catalogue of Tsunamis for the New Guinea/Solomon Islands Region, 1768–1972,* Bureau of Mineral Resources, Geology, and Geophysics Report 180, Canberra, 78 pp.

Geist, E. L. (2002). Complex earthquake rupture and local tsunamis, Journal of Geophysical Research **107**(B5), ESE2-1 – ESE2-16.

Geller, R. J. (1976). Scaling relations for earthquake source parameters and magnitudes, *Bulletin of the Seismological Society of America* **66**, 1,501–1,523.

Gutenberg, B. and C. F. Richter (1954). *Seismicity of the Earth and Associated Phenomena,* Princeton, NJ: Princeton University Press, 310 pp.

Heinrich, P., A. Piatanesi, E. A. Okal, and H. Hébert (2000). Near-field modeling of the July 17, 1998 tsunami in Papua New Guinea, *Geophysical Research Letters* **27**, 3,037–3,040.

Hoffman, I., C. E. Synolakis, and E. A. Okal (2002). Systematics of the distribution of tsunami run-up along coastlines in the near-field for dislocation sources with variable parameters, *Eos, Transactions of the American Geophysical Union* **83**, WP54 (abstract).

Johnson, R. W. and P. Molnar (1972). Focal mechanisms and plate tectonics of the Southwest Pacific, *Journal of Geophysical Research* **77**, 5,000-5,032.

Kagan, Y. Y. (1991). 3-D rotation of double-couple earthquake sources, *Geophysical Journal International* **106**, 709–716.

Kawata, Y., B. C. Benson, J. C. Borrero, J. L. Borrero, H. L. Davies, W. P. de Lange, F. Imamura, H. Letz, J. Nott, and C. E. Synolakis (1999). The July 17, 1998, Papua New Guinea earthquake and tsunami, *Eos, Transactions of the American Geophysical Union* **80**, 101.

Neuhauss, R. (1911). *Deutsch Neu-Guinea*, 3 volumes, Berlin: Dietrich Reimer.

Newman, A. V. and E. A. Okal, Teleseismic estimates of radiated seismic energy: The E/M_0 discriminant for tsunami earthquakes, *Journal of Geophysical Research* **103**, 26,885–26,898.

Okada, Y. (1985). Surface deformation due to shear and tensile faults in a half-space, *Bulletin of the Seismological Society of America* **75**, 1,135–1,154.

Okal, E. A. (2003). *T* waves from the 1998 Papua New Guinea earthquake and its aftershocks: Timing the tsunamigenic slump, *Pure and Applied Geophysics* **160** (in press).

Okal, E. A., L. Dengler, S. Araya, J. C. Borrero, B. Gomer, S., Koshimura, G. Laos, D. Olcese, M. Ortiz, M. Swensson, V. V. Titov, and F. Vegas (2002). A field survey of the Camana, Perú tsunami of June 23, 2001, *Seismological Research Letters* **73**, 904–917.

Okal, E. A. and J. Talandier (1990). M_m: Extension to Love waves of the concept of a variable-period mantle magnitude, *Pure and Applied Geophysics* **134**, 355–384.

Solov'ev, S. L., Ch. N. Go, and Kh. S. Kim (1986). *Katalog tsunami v tikhom okeane, 1969–1982 gg.*, Moskva: Akad Nauk SSSR, 164 pp.

Sweet, S. and E. A. Silver (2003). Tectonics and slumping in the region of the 1998 Papua New Guinea tsunami from seismic reflection images, *Pure and Applied Geophysics* **160** (in press).

Synolakis, C. E., J.-P. Bardet, J. C. Borrero, H. L. Davies, E. A. Okal, E. A. Silver, S. Sweet, and D. R. Tappin (2002). The slump origin of the 1998 Papua New Guinea tsunami, *Proceedings of the Royal Society (London), Series A* **458**, 763–789.

Tappin, D. R., T. Matsumoto, P. Watts, K. Satake, G. M. McMurtry, M. Matsuyama, Y. Lafoy, Y. Tsuji, T. Kanamatsu, W. Lus, Y. Iwabuchi, H. Yeh, Y. Matumotu, M. Nakamura, M. Mahoi, P. Hill, K. Crook, and L. Anton (1999). Sediment slump likely caused 1998 Papua New Guinea tsunami, *Eos, Transactions of the American Geophysical Union* **80**, 329, 334, 340.

Titov, V. V. and F. Gonzalez (1997). Implementation and testing of the Method Of Splitting Tsunami (MOST) Model, *NOAA Technical Memorandum ERL PMEL – 112.*

Titov, V. V. and C. E. Synolakis (1998). Numerical modeling of tidal wave runup, *Journal of Waterways, Port, Coastal and Ocean Engineering* **124**, 157–171.

Toppozada, T. R. (1975). Earthquake magnitude as a function of intensity data in California and Western Nevada, *Bulletin of the Seismological Society of America* **65**, 1,223–1,238.

Tregoning, P. (2002). Plate kinematics in the Western Pacific derived from geodetic observations, *Journal of Geophysical Research* **107**(B1), ECV 7-1 – ECV 7-8.

Tsuji, Y., F. Imamura, H. Matsutomi, C. E. Synolakis, P. T. Nanang, Jumadi, S. Harada, S. S. Han, K. Arai, and B. Cook (1995). Field survey of the East Java earthquake and tsunami of June 3, 1994, *Pure and Applied Geophysics* **144**, 839–854.

Wessel, P. and W. H. F. Smith (1991). Free software helps map and display data, *Eos, Transactions of the American Geophysical Union* **72,** 441, 445–446.

Wysession, M. E., E. A. Okal, and K. L. Miller (1991). Intraplate seismicity of the Pacific Basin, 1913–1988, *Pure and Applied Geophysics* **135**, 261–359.

Department of Civil Engineering
University of Southern California
Los Angeles, CA 90089, USA
(J.C.B., B.U., C.E.S.)

Department of Geology
University of Papua New Guinea
Port Moresby
Papua New Guinea
(J.B., C.S.)

Marine Facilities Division
California State Lands Commission
Long Beach, CA 90802, USA
(J.F.)

Department of Geological Sciences
Northwestern University
Evanston, IL 60201, USA
emile@earth.nwu.edu
(B.G., E.A.O.)